INSTABILITY CAUSED BY ELECTRON CLOUD IN COMBINED FUNCTION MAGNETS: THE FERMILAB EXPERIENCE

S. A. Antipov, CERN, Geneva, Switzerland

Abstract

Electron cloud can lead to a fast instability in intense proton and positron beams in circular accelerators. In the Fermilab Recycler the electron cloud is confined within its combined function magnets. We show that the field of combined function magnets traps the electron cloud, present the results of analytical estimates of trapping, and compare them to numerical simulations of electron cloud formation. The electron cloud is located at the beam center and up to 1% of the particles can be trapped by the magnetic field. Since the process of electron cloud build-up is exponential, once trapped this amount of electrons significantly increases the density of the cloud on the next revolution. In a Recycler combined function dipole this multi-turn accumulation allows the electron cloud reaching final intensities orders of magnitude greater than in a pure dipole. The multi-turn build-up can be stopped by injection of a clearing bunch of 10^{10} p at any position in the ring.

FAST INSTABILITY

In 2014 a fast transverse instability was observed in the proton beam of the Fermilab Recycler. The instability acts only in the horizontal plane and typically develops in about 20-30 revolutions. It also has the unusual feature of selectively impacting the first batch above the threshold intensity of $\sim 4\times10^{10}$ ppb (Fig. 1). The instability is triggered by longitudinal bunch compression (Fig. 2) that occurs due to bunch rotation at injection. These peculiar features suggest that a possible cause of the instability is electron cloud.

Early studies [1,2] indicated the presence of electron cloud in the ring and suggested the possibility of its trapping in Recycler combined function magnets. The presence of the cloud has also been observed in the Main Injector (MI) [3], which operates with similar beams, but it has never caused stability issues. The major difference between the MI (at the injection energy) and the Recycler seems to be the choice of technology for their dipole magnets: separate function (MI) vs combined function (Recycler).

The fast instability seems to be severe only during the start-up phase after a shutdown, with significant reduction being observed after beam pipe conditioning during beam scrubbing runs [4]. It does not limit the current operation with slip-stacking up 700 kW of beam power, but may pose a challenge for a future PIP-II intensity upgrade.

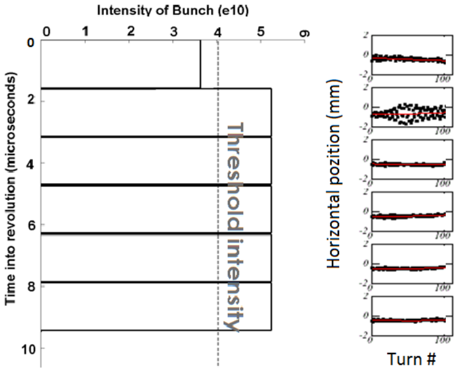

Figure 1: The first batch above the threshold intensity suffers the blow-up after injection into the ring [4].

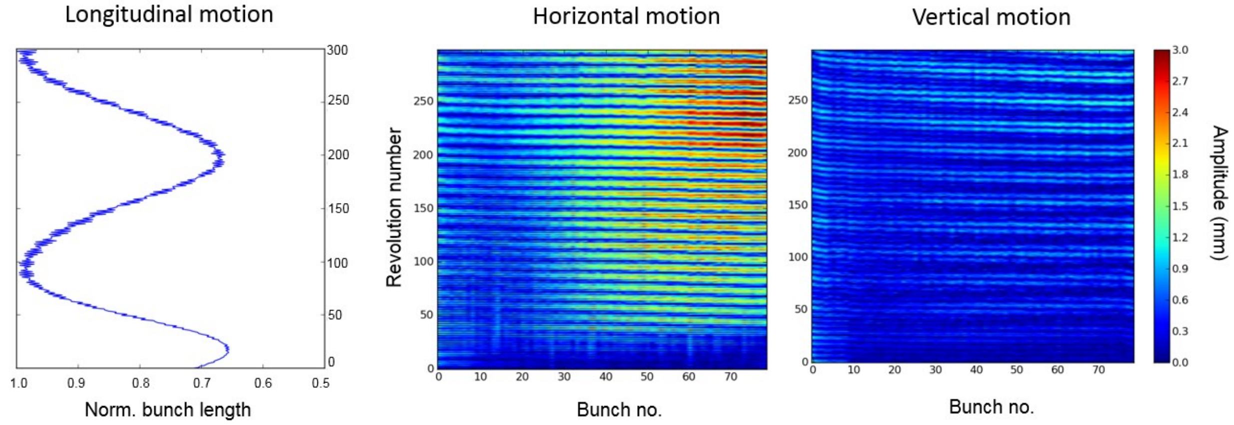

Figure 2: The instability mostly affects the last bunches in the train. It starts after the beam compresses longitudinally (left) and then becomes more severe after it compresses again, half a synchrotron period later. The color depicts the amplitude of the horizontal betatron oscillations of the beam center of mass as a function revolution number and position within the batch. The horizontal stripes are caused by our sampling of beam position once a revolution and appear at twice the betatron frequency: $2Q_x = 0.9$ or 1/10 turns. The data was gathered over 300 revolutions with the transverse dampers off. Beam: 1 batch, 80 bunches, 5×10^{10} ppb.

ELECTRON CLOUD TRAPPING

In a combined function dipole the electrons of the cloud move along the vertical field lines. This motion conserves their energy E and magnetic moment

$$\mu = \frac{mv_\perp^2}{2B} = const, \tag{1}$$

where $v_\perp$ is the component of the velocity normal to the magnetic field B. As an electron moves closer to a magnet pole it sees a higher B (Fig. 2) and it can reflect back if

$$E - \mu B = 0 \tag{2}$$

Alternatively, the electron will reflect back at the point of maximum magnetic field if the angle between the electron's velocity and the field lines is greater than:

$$\theta > \theta_{\max} = \cos^{-1}(\sqrt{B_0 / B_{\max}}). \tag{3}$$

Particles with angles $\theta_{\max} < \theta \leq \pi / 2$ are trapped by magnetic field. For Recycler magnets (Table 1), Eq. (3) gives a capture of ~10^{-2} particles of electron cloud, assuming uniform distribution.

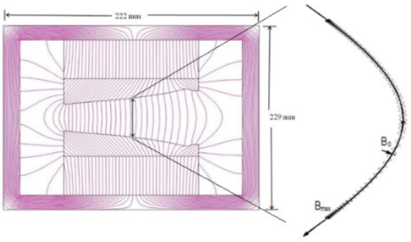

Figure 3: Electron cloud can get trapped by magnetic field of a combined function magnet.

Lifetime of the trapped cloud

Long-term confinement of the electron cloud can be affected by two effects: longitudinal drift and scattering. The drift is caused by the absence of magnetic field gradient in the longitudinal direction. The longitudinal drift velocity can be estimated as

$$v_d = \frac{1}{2}\omega_c r_c^2 \frac{B'}{B_0}, \tag{5}$$

where ω_c is the cyclotron frequency and r_c – the radius of the orbit. In the Fermilab Recylcer an electron cloud particle travels less than 2 cm during on beam revolution, much smaller than the length of its magnets. The drift can therefore be neglected.

The Coulomb scattering cross-section is

$$\sigma_C = \frac{4\pi}{9}\frac{e^4 \ln \Lambda}{(\mathrm{kT})^2} \sim 10^{-15}\mathrm{cm}^2 \tag{6}$$

The inelastic scattering cross-section for the energies in question is also of the order of $10^{-15}\mathrm{cm}^2$ [5]. Combining the two effects we obtain a lifetime ~ 10 ms for the electron cloud density $n_e < 10^7$ cm^{-3} and the residual gas pressure p ~ 10^{-8} Torr. Since the resulting lifetime of the electron cloud is much larger than the revolution period of 11 µs, all the trapped cloud will be present on the next turn.

Electron cloud clearing with a witness bunch

As mentioned above, the trapping requires at least two bunches: the first to kick the cloud and create the secondaries; and the second to stop a fraction of those. Therefore, a single bunch of high enough intensity does not trap the cloud but clears the aperture instead. This clearing bunch can be used to indicate the presence of the trapped electron cloud and measure its density [6] or to bring the electron cloud density below the threshold, stabilizing the beam.

NUMERICAL SIMULATION OF ELECTRON CLOUD BUILD-UP

We simulated electron cloud build-up over multiple revolutions in a Recycler dipole using the PEI code [7]. For a pure dipole field, the cloud rapidly builds up during the passage of the bunch train and then decays back to the initial ionization electron density in about 300 RF buckets, or ~ 6 µs (Fig. 6). When the field gradient is added, up to 1% of the electron cloud stays trapped, increasing the initial density on the next revolution. The final density, which the cloud reaches after ~ 10 revolutions, is two orders of magnitude greater than in the pure dipole case (Fig. 4). The resulting cloud distribution is a stripe along the magnetic field lines, with higher particle density being closer to the walls of the vacuum chamber (Fig. 5). The width of the stripe is approximately equal to the size of the beam and its intensity increases from turn to turn as the cloud builds up.

At lower densities ~10^{-2} of particles are trapped, which agrees with the analytic estimate (Fig. 4); as the density of electron cloud increases the trapping ratio goes down to ~10^{-3}, probably due to the space charge of electron cloud.

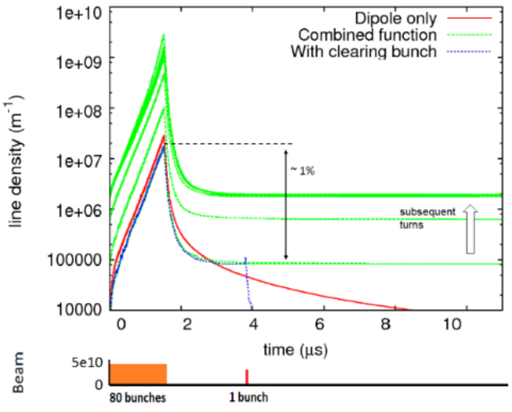

Figure 4: In a combined function magnet the electron cloud accumulates over many revolutions, reaching much higher line density, than in a dipole. A clearing bunch destroys the trapped cloud, preventing the accumulation.

A bunch of 5×10^{10} protons, added 120 RF buckets after the main batch, destroys the trapped cloud, preventing the multi-turn build-up (Fig. 4). First, one can see a small increase in the cloud density as the clearing bunch kicks the cloud and it reaches the vacuum chamber, producing the secondary electrons. Then, the density rapidly drops as these secondaries reach the aperture.

Table 1: Recycler parameters for simulation in PEI

Beam energy	8 GeV
Machine circumference	3.3 km
Batch structure	80 bunches, 5×10^{10} p
Tunes: x, y, z	25.45, 24.40, 0.003
RF harmonic, period	588; 18.9 ns
RMS bunch size: x, y, z	0.3, 0.3, 60 cm
Secondary emission yield	2.1 @ 250 eV
Density of ionization e$^-$	10^4 m^{-1} (at 10^{-8} Torr)
B-field and its gradient	1.38 kG, 3.4 kG/m
Magnet length	5 m
Beampipe	Elliptical, 100 x 44 mm

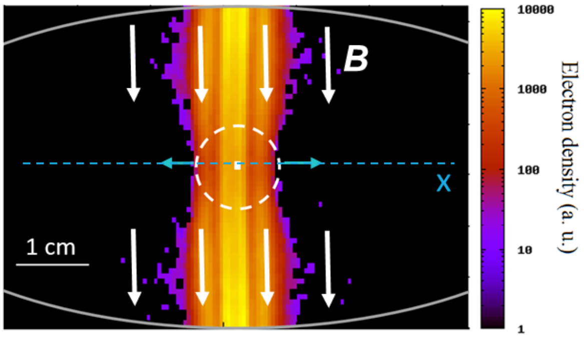

Figure 5: Electron cloud forms a stripe inside the vacuum chamber and its intensity increases with the number of turns. Its horizontal position – beam center (white dot). White circles represent 2 rms beam size.

ANALYTICAL MODEL

As a reactive medium, the electron cloud interacts with the beam similarly to a low-Q impedance [8-10]. Electron cloud instability in the presence of a strong magnetic field can also be calculated using assumptions about the shape of the wake as in [11]. Here we study the beam-cloud motion in a strong dipole field, modelling the motion of the cloud 'stripe' as the mobility term, similar to the work [12]. This approach does not require making initial assumptions about the form of the electron cloud wake or its impedance.

First, consider a round coasting proton beam travelling in a ring with the beam centroid position at an azimuthal angle θ and time t being $X_p(t, \theta)$. Further, assume that the beam travels at a constant azimuthal velocity around the ring ω_0 and use a smooth focusing approximation with a betatron frequency ω_β. For simplicity, one can assume that the ring is uniformly filled with electron cloud of a constant density n_e, which forms a column of the same transverse size as the proton beam, and is located at a horizontal position X_e. Because of the vertical dipole field, the individual electrons of the cloud cannot drift horizontally, but the position X_e can change as some regions build up and others decay, following the transverse motion of the proton beam (Fig. 5). The characteristic rate of this slow motion of the electron cloud λ is then the rate of its build-up: $\lambda \sim 1/\tau_{buildup}$.

For small oscillation amplitudes we can assume the electron-proton interaction force to be linear in displacement. Then the coupled collective motion of the beam and the electron cloud is described by the following system of equations:

$$\begin{cases} \frac{d^2}{dt^2}X_p + \Gamma\frac{d}{dt}X_p = -\omega_\beta^2 X_p + \omega_p^2(X_e - X_p), \\ \frac{\partial}{\partial t}X_e = \lambda(X_e - X_p), \end{cases} \qquad (7)$$

where d/dt stands for $(\partial/\partial t + \omega_0\partial/\partial\theta)$, Γ is the rate of Landau damping defined below and the coupling frequency ω_p is approximated as

$$\omega_p^2 = 2\pi n_e r_p c^2/\gamma \qquad (8)$$

where r_p is the classical proton radius and γ – the relativistic factor. The linear damping term Γ in Eq. (7) arises from the spread in betatron frequencies for particles oscillating with different amplitudes. The characteristic rate of the Landau damping can be estimated as

$$\Gamma \sim \omega_\beta \Delta Q_x / Q_x, \qquad (9)$$

where Q_x is the horizontal tune and ΔQ_x is its rms spread.

Looking for solutions of Eq. (7) in a form $X_{e,p} \propto \exp[-i(\omega t - k\theta)]$, where $\omega = k\omega_0 + \omega_\beta + \Delta\omega$ and k is an integer mode number, one obtains an equation for the complex mode frequency shift:

$$\Delta\omega \approx \frac{1}{2}\left[-i\Gamma + \frac{\omega_p^2}{\omega_\beta}\frac{\omega(\omega - i\lambda)}{\lambda^2 + \omega^2}\right] \qquad (10)$$

The most unstable mode with the largest growth rate $\gamma = \mathrm{Im}(\Delta\omega)$, corresponds to a wave number

$$k_{\max} = \lambda/\omega_0 - Q_x. \qquad (11)$$

The tune shift of this mode is

$$\Delta Q_{\max} \approx \frac{1}{4Q_x}\frac{\omega_p^2}{\omega_0^2}. \qquad (12)$$

The threshold electron cloud density $n_{e,thr}$ can be found from the condition $\gamma_{max} = 0$, which yields

$$n_{e,thr} = \gamma\omega_\beta\Gamma/\pi r_p c^2. \qquad (13)$$

Note that in this simple model we do not consider the electron cloud's contribution to Landau damping, which may arise from the nonlinear spread of the betatron tunes, created by the cloud.

Knowing the complex frequency shift $\Delta\omega$ we can find the impedance of the cloud as (see for example [13] Eq. (6.262)):

$$Z(\omega) = iZ_0\frac{\gamma T_0^2\omega_\beta}{2\pi N r_p}\Delta\omega, \qquad (14)$$

where N is the number of protons in the ring and Z_0 is the vacuum impedance.

In the case of a bunched beam, in a rigid bunch approximation with the bunch spacing of τ_{rf} , one can use the impedance of the most unstable mode $Z_{\max} = \mathrm{Re}[Z(\omega_{\max})]$ to compute its growth rate (for derivation see [14]):

$$\gamma_{b,\max} \approx \frac{L}{C}\frac{8\pi r_p N_b \beta_x}{\gamma c \tau_{rf}}\frac{Z_{\max}}{Z_0} - \frac{\Gamma}{2}, \qquad (15)$$

where C is the ring circumference and L is the total length of the magnets. For the Recycler $L/C \approx 1/2$.

Instability in Recycler

In order to use the model and estimate the parameters of the fast instability in Recycler one needs to know the density of the electron cloud and the rate of its build-up. We obtained these quantitative parameters by measuring the betatron frequency shift and comparing it with the build-up simulations. We injected one batch of 80 proton bunches of 5×10^{10} ppb and measured the shift of the horizontal tune as a function of bunch number. Because the positive horizontal tune shift is a distinctive feature of the electron cloud, it allowed us an estimation of the cloud density. In order to check with the simulation the cloud density both within the high-intensity batch and after its passage we put a witness bunch of low intensity -0.8×10^{10} p, insufficient to clear the electron cloud, at different positions behind the main batch.

The experimental results are in good agreement with the simulation (Fig. 6) and the small discrepancies may come from the multiple assumptions used in Eq. (15). The resulting dependence allows the estimation of the maximum density of electron cloud $n_e \sim 6\times10^{11}$ m^{-3}. The density increases by an order of magnitude in 40 bunches (800 ns) and falls after the beam has passed in 10 bunches (200 ns). The characteristic rate of the exponential build-up is 2.65×10^{6} s^{-1}.

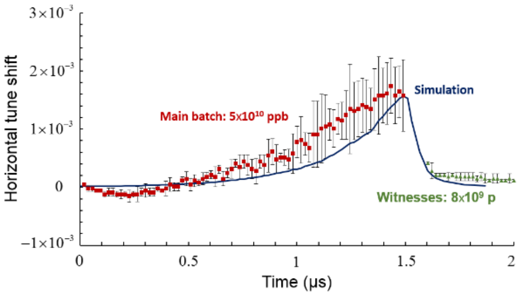

Figure 6: Results the of electron cloud simulation agree with the measured horizontal tune shift. Beam: 5×10^{10} ppb, 80 bunches, followed by one witness bunch of 0.8×10^{10} p at various positions. The gap between the high-intensity batch and the witness is due to the rise-time of the injection kickers.

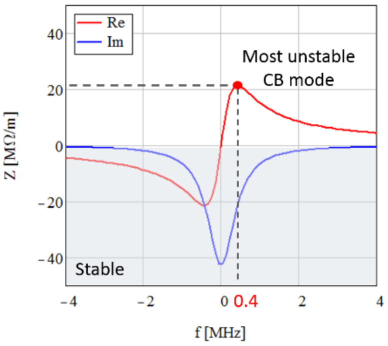

Figure 7: Real and imaginary parts of impedance as a function of a mode angular frequency ω.

Figure 7 shows an effective electron cloud impedance corresponding to the estimated cloud density, estimated using Eq. (14). Using Eq. (15) we obtain the growth rate of 3.3×10^{-2} and the characteristic time of the instability of around 30 turns for a bunch intensity of 5×10^{10} ppb. The threshold electron cloud density, calculated using Eq. (13), $n_{e,thr} = 8.2\times10^{10}$ m^{-3}. According to numerical build-up simulations, this density is achieved at the proton intensity of about 4.5×10^{10} ppb, which is also consistent with experimental observations.

CONCLUSION AND OUTLOOK

Combined function magnets are widely used in the present day machines. Because of the gradient of the magnetic field (which provides the focusing) the electron cloud can be trapped in the magnetic field of such magnets. These trapped particles make it possible for the cloud to accumulate over multiple revolutions, possibly leading to a fast transverse instability.

We have created an analytical model that allows the estimation of the amount of the cloud captured in the magnet. We have shown that up to 1% of the electron cloud can be trapped in the magnetic field of combined function magnets of FNAL Recycler. This fraction of trapped particles will go down for higher intensities in Recycler.

Numerical simulation in PEI agrees with the analytical estimate and confirms that the trapping significantly affects the density of the electron could. It allows the cloud to accumulate over multiple revolutions reaching a density much higher than in a pure dipole. For the parameters of Fermilab Recycler with one batch of normal intensity the cloud reaches ~ 10^{9} m^{-1} in a combined function magnet compared to ~ 10^{7} m^{-1} in a dipole of the same field strength. An addition of a clearing bunch destroys the trapped cloud, preventing the multi-turn accumulation.

An instability similar to Recycler one occurs in the CERN PS, which also utilizes combined function magnets. The instability was observed in operation before extraction when bunch length is compressed from 11 to 4 ns and in a dedicated study where the beam was stored for a long time – 100 ms at 11 ns bunch length [15,16]. The instability does not limit the operational performance since normally the beam does not interact with the cloud for a sufficiently long time. Although the trapped cloud might play a minor role in the PS role thanks to the fact that nearly all machine is full, leaving little time for the cloud to decay before the next revolution. A thorough analysis may be needed to identify at which parameters the trapped cloud can pose a limitation.

ACKNOWLEDGMENT

This work was performed as a part of PhD thesis research at Fermilab. The author is grateful numerous members of Fermilab Accelerator Division for their contribution t they study and especially to the PhD advisor S. Nagaitsev, and would also like to thank K. Ohmi (KEK) for his help with PEI code. Fermilab is operated by Fermi Research Alliance, LLC under Contract No. DE-AC02-07CH11359 with the United States Department of Energy.

REFERENCES

[1] J. Eldred, *et al.*, in *Proc. HB'14,* pp. 419-427, 2014
[2] S. A. Antipov, et al., in *Proc. IPAC'16*, pp. 1728-1730
[3] N. Eddy *et al.*, in *Proc. PAC'09,* 2009
[4] J. Eldred, "The High-Power Recycler: Slip-stacking & Electron Cloud", Fermilab, Nov. 2015
[5] A. D. MacDonald, *Microwave Breakdown in Gases*, New York, NY: Wiley, 1966
[6] M. Billing *et al., Phys. Rev. ST Accel. Beams* vol. 18, p. 041001, Apr. 2015
[7] K. Ohmi, CERN Rep. CERN-2013-002, pp.219-224
[8] K. Ohmi and F. Zimmermann, *Phys. Rev. Lett.* vol. 85, pp. 3821–3824, 2000
[9] K. Ohmi, F. Zimmermann, and E. Perevedentsev, *Phys. Rev. E* vol. 65, p. 016502, 2001
[10] A. Burov, FERMILAB-PUB-13-005-AD, 2013
[11] V. Balbekov, FERMILAB-FN-1001-APC, 2015
[12] G. Arduini *et al.*, in *Proc. PAC'03*, pp. 3038-3040, 2003
[13] A. Chao, *Physics of Collective Beam Instabilities in High Energy Accelerators*, Ney York, NY: Wiley, 1993
[14] Yu. Alexahin, FNAL Beams-doc-4863-v1, 2015
[15] R. Cappi *et al., Phys. Rev. ST Accel. Beams* vol. 5, 2002
[16] G. Iadarola *et al.*, in *Proc. IPAC'13*, 2013